Journal of Crystal Growth 542 (2020) 125670

Contents lists available at ScienceDirect

Journal of Crystal Growth

journal homepage: www.elsevier.com/locate/jcrysgro

The effect of preliminary heat treatment on the durability of reaction bonded silicon nitride crucibles for solar cells applications

Rania Hendawi[a,*], Arjan Ciftja[b], Gaute Stokkan[c], Lars Arnberg[a], Marisa Di Sabatino[a]

[a] Department of Materials Science and Engineering, NTNU, 7491 Trondheim, Norway
[b] Steuler Solar Technology, 3905 Porsgrunn, Norway
[c] SINTEF Industry, 7465 Trondheim, Norway

ARTICLE INFO

Communicated by P. Rudolph

Keywords:
A1. Crucible cracking
A1. Heat treatment
A1. Characterization
B1. Nitrides

ABSTRACT

Silicon nitride crucibles have the potential to replace silica crucibles and reduce the cost of silicon crystallization because of their reusability potential. Till date, crucibles' heat treatment before each use is a prerequisite to achieve non-wetting conditions that is needed to facilitate the ingot release and hence enable reusability. Yet, no studies have examined the heat treatment influence on the crucibles' durability. The present investigation focuses on the crucibles' heat treatment and its impact on the crucibles' lifetime. Repeated heat-treatments of silicon nitride crucibles in the air at above 1100 °C leads to crucible fracture. Therefore, this study identifies the cause and the mechanism of such failures by applying different heat treatment procedures in the air. The mass gain and the oxidation rates of the crucibles at different temperatures are measured via Thermogravimetry (TG) and Differential Thermal Analyzer (DTA). The results show that the porosity and phase distribution along the crucible wall thickness, play a key role in the crucible's behavior during oxidation. Moreover, excessive internal oxidation in the tested crucibles results in severe thermal stresses which cause cracking during cooling.

1. Introduction

Crucibles contribute significantly to the multi-crystalline silicon ingots in terms of cost and quality [1–3]. To date, silica is the material of choice due to its availability, high melting temperature, and purity. Yet the major drawbacks of silica are; (i) its reactivity with molten silicon which results in a high oxygen content that negatively affects the efficiency of the solar cell and, (ii) its single-use by virtue of the crucible cracking during cooling as a result of the two-phase transformations that silica crucibles undergo.

Silicon nitride has the potential to replace silica crucibles owing to its low thermal expansion, chemical stability and comparable purity. The significance of silicon nitride crucibles to the future of PV market lies in its reusability and low oxygen content. Both attributes can reduce silicon production cost and yield high-efficiency solar cells. Over the past two decades, a number of patents claimed the reusability of silicon nitride crucibles and their manufacturing processes [4,5]. Subsequently, some studies reported the effectiveness of silicon nitride crucibles in multi-crystalline Si ingots growth in terms of cost and contamination level [1,6]. For example, Bellmann et al. [1] reported lower oxygen and metallic impurities levels in silicon nitride crucible ingots compared to high purity electronic-grade silica crucibles.

Fig. 1 illustrates the lifecycle of a silicon nitride crucible. Traditionally, after cleaning, silicon nitride crucibles are coated with a high purity silicon nitride layer to facilitate the ingot removal upon solidification and act as a diffusion barrier during melting. At the next stage of the process, heat treatment is performed to oxidize the coating and enhance its cohesion. Studies have shown that the heat treatment step is crucial to avoid wetting of coating by molten silicon which may cause cracks in the ingot and the crucible [7,8]. Following the heat treatment, the crucible is used for silicon solidification and ingot is released subsequently. The crucible then undergoes the same preparation process for the next solidification run.

In this study, we use the reaction bonded silicon nitride crucibles which are processed without using sintering aids or permanent binders to ensure the high purity of the crucibles which is critical for the solar applications. Reaction bonded silicon nitride (RBSN) was firstly developed in the middle of the last century via the nitridation of silicon powder at temperature below its melting point [9]. The process results in a material with density 70–80% of the theoretical density of Si_3N_4, and a porosity volume fraction up to 25% [9]. In principle, a low thermal expansion coefficient and therefore high thermal shock resistance of RBSN [10], ensure the crucible durability over several thermal cycles particularly during both heat treatments and

* Corresponding author.
E-mail address: rania.hendawi@ntnu.no (R. Hendawi).

https://doi.org/10.1016/j.jcrysgro.2020.125670
Received 24 March 2020; Received in revised form 10 April 2020; Accepted 11 April 2020
Available online 21 April 2020

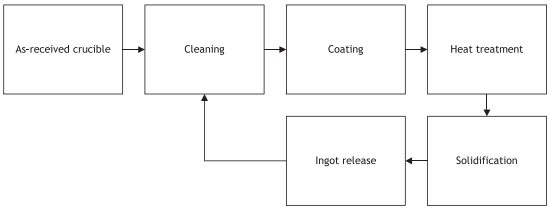

Fig. 1. Schematic drawing of the silicon nitride crucible lifecycle.

solidification runs. The major concern during solidification, which takes place in an argon atmosphere, is to avoid the wetting of silicon nitride crucible by molten silicon which, if it occurs, will make it difficult to release the solidified silicon ingot and hence, prohibit crucible reusability. Regarding the heat treatment step that requires the oxidation at 1100 ˚C, it is crucial to understand the oxidation behavior of silicon nitride crucibles at this temperature especially that heat treatment must be performed before each solidification run. Several studies [8,11] addressed the wetting of silicon nitride during solidification, however little attention has been paid on the heat treatment of the silicon nitride crucibles which is an essential step for non-wetting conditions.

The present paper aims to better understand the oxidation behavior of the crucibles during the heat treatment and its influence on crucibles lifetime. The study also investigates the influence of the silicon nitride properties such as the porosity and the phase distribution on the oxidation behavior and the durability of the crucibles.

2. Experimental

Experiments are performed on reaction bonded silicon nitride (RBSN) crucibles supplied by Steuler Solar Technology. Crucibles of two different porosities are investigated as listed in Table 1. The crucibles are produced by a novel slip casting technique followed by a nitridation process at high temperatures. The production steps can be summarized as follows:

(i) A slurry of high purity silicon powder, water and binders is prepared and stabilized until constant characteristics are achieved.
(ii) The slurry is poured in one-sided plaster mold that extracts liquid from the slip by capillary action. The excess slurry is drained upon the desired thickness is built up.
(iii) The cast (greenware) is removed from the mold after partial drying.
(iv) After complete drying, nitridation of the casts occurs above 1000 ˚C and final RBSN crucibles are produced.

Throughout this paper, the term “oxidation cycle or heat treatment” will refer to one complete test which includes; (i) heating the crucible to the desired oxidation temperature (Tox), (ii) holding two hours at Tox, and (iii) cooling to the room temperature. The crucibles are subjected to oxidation cycles at temperatures ranging from 900 to 1200 ˚C in air atmosphere with a heating rate of 100 ˚C/hr. Two sets of heat treatment experiments are conducted: (i) heat treatment of coated crucibles at 1100 ˚C and (ii) heat treatment of uncoated crucibles at 900 to 1200 ˚C.

Table 1
Characteristics of RBSN crucibles.

	Type A	Type B
Bulk density (g/cm^3)	2.551	2.359
Open porosity (vol%)	14.7	23.9
True porosity (vol%)	20.1	26.1
Thickness (mm)	6.9 ± 0.3	6.9 ± 0.3
Diameter (mm)	250	270
α /β-Si_3N_4 ratio	70/30	70/30

For the coating preparation, a slurry composed of α-Si_3N_4 powder and binder, polyvinyl alcohol, is first prepared. The coating is applied to the inner surface of the crucibles by spraying.

Porosity and density measurements are performed by Archimedes immersion technique in isopropanol and image analysis method. The oxidation degree is measured by means of oxygen compositional profile, oxide compounds content and mass gain of the tested samples. Thermal gravimetric analysis (TGA) is carried out using on LINSEIS STA PT1600 with a heating rate of 10 ˚C/min and airflow of 100 cm^3/min. JEOL JXA-8500F Electron Probe Microanalyzer is used to evaluate the compositional profiles of oxygen of preoxidized samples that are precoated with a thin carbon layer to enhance the conductivity of the surface and avoid charging. A Bruker D8 A25 DaVinci X-ray Diffractometer with CuKα radiation is used for phase composition analysis of the samples and DIFFRAC.TOPAS 5.0. is used for data refinement and quantitative analysis. Secondary electron images, backscattered electron images, and EDS analysis are performed using a LV-Fe-SEM (Zeiss Supra 55 VP).

3. Results and discussions

3.1. Heat treatment

The heat treatment experiments on coated crucibles at 1100 ˚C lead to: (i) severe cracking in type B crucibles upon the third oxidation cycle, (ii) slight cracks in type A upon the eightieth oxidation cycle. Type A shows higher tolerance in the oxidizing atmosphere. Therefore, the second series of experiments is conducted on uncoated crucibles, type B, to determine the possible implication of the coating to the crucible cracking and investigate the oxidation influence on the entire crucible. The uncoated crucibles also experience severe cracking during the oxidation tests. Fig. 2 provides an overview of the type B tolerance to failure, oxidation cycles to failure, at different oxidation temperatures. In fact, the crucibles tendency to failure increases drastically with the oxidation temperature which in turn may reflect the oxidation degree. As an example, heat treating the silicon nitride crucible at 900 ˚C instead of 1200 ˚C will increase up the times to failure by factor of five. Considering the above, the heat treatment step seems to limit the reusability of the crucibles. Therefore, a thorough investigation of the failure causes and their relation to the crucible properties will be discussed in the following sections.

3.2. Fractographic examination

It is important to determine whether the failure is due to a thermal shock, which refers to thermal stresses associated with a sudden change in temperature, or due to the oxidation that results from heating in air atmosphere. For this intention, another set of experiments is conducted by heating the crucibles in an argon atmosphere up to 1500 ˚C. The crucibles sustain the repeated heating cycles up to 1500 ˚C in argon atmosphere and no cracking is observed. Yet heating in air atmosphere

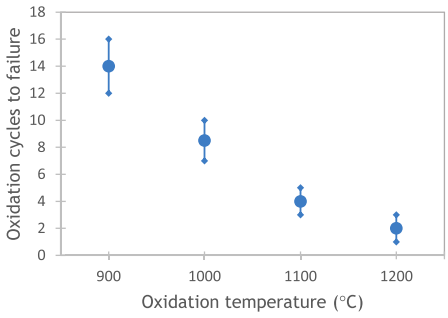

Fig. 2. Number of oxidation cycles to failure at different oxidation temperatures for uncoated type B crucibles.

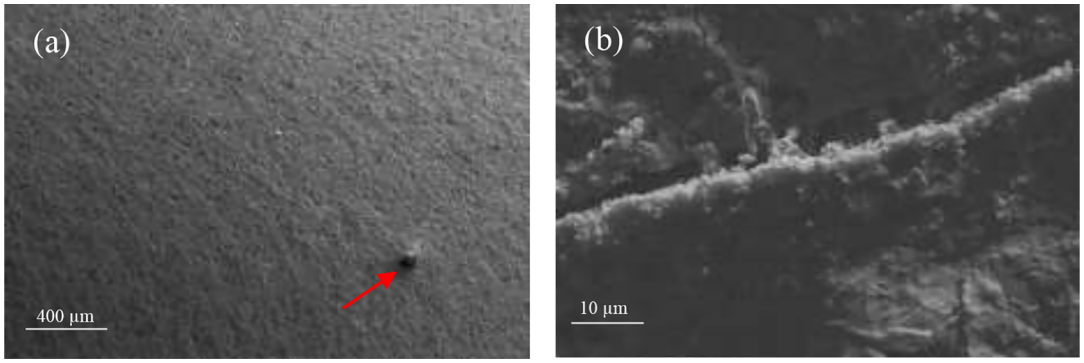

Fig. 3. SEM micrographs of the B crucible fracture surface: (a) material flaw; (b) micro crack at the fracture surface. No special fracture features observed.

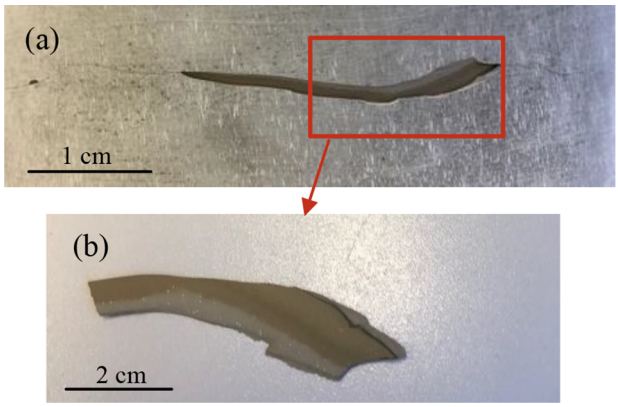

Fig. 4. Cracking of crucible type B upon the heat treatment : (a) cracking and peeling of the outer surface; (b) the peel geometry (0.72 mm thickness).

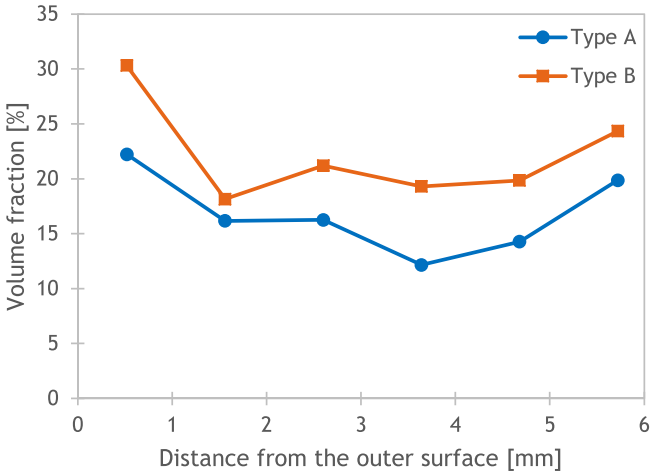

Fig. 5. Porosity volume fraction along thickness for both crucible types.

leads to severe cracking of the crucibles. The in-situ observation of the crucibles during the heat treatments in oxidizing atmosphere reveals that crucibles crack during cooling, when the temperature is lower than 200 °C. The investigations of the fracture surface via electron microscopy reveal some microcracks as well as material flaws as shown in Fig. 3, however, no special fracture features are spotted in the vicinity. This implies that there is no crucial role of the material flaws on the cracks' initiation, though, they still may affect the crack propagation. In the light of the above, oxidation of the silicon nitride crucibles contributes significantly to the failure of silicon nitride crucibles, and further examination of the fractures in needed to determine how the oxidation causes this failure and its relationship to the crucible and application conditions. Another key question is why this failure occurs upon a short period of oxidation despite the researches that claim the RBSN durability in oxidizing atmosphere up to 3000 operating hours [12]. Visual examination and reconstruction of the fractured pieces show that cracks initiate on the outer surface of type B and resulted in detachment and of the outer surface of the crucible wall in some regions as illustrated in Fig. 4. The fracture also reveals color gradient across the crucible thickness. Phase analysis and porosity measurements of these observed layers are presented in the following section.

3.3. Porosity and phase analysis across thickness

In this paper, there are two types of RBSN crucibles with differences in the apparent and true porosities. Yet this is not the only difference between both types, crucibles A show higher durability during heating in air atmosphere. By subjecting both types to the same heat treatment conditions, cracking is only observed on type B. Therefore, the upcoming investigations are conducted on both types to identify the reasons behind type B behavior. Archimedes immersion technique shows that type A has lower porosities, open and overall, than type B. Image analysis for the optical images across the crucibles thickness agrees with Archimedes values and provides more details on the porosity distribution across the crucibles thickness as presented in Fig. 5. Unlike in type A, besides the high porosity value, a sharp gradient in the porosity can be seen at approximately 1 mm distance from the outer surface in type B.

The overall composition is investigated via XRD for both types upon oxidation at 1200 °C . The major oxidation reactions of silicon nitride are represented as the following:

$$Si_3N_{4(s)} + 3O_{2(g)} \leftrightarrow 3SiO_{2(s)} + 2N_{2(g)} \quad (1)$$

$$Si_3N_{4(s)} + \frac{3}{2}O_{2(g)} \leftrightarrow 3Si_2ON_{2(s)} + N_{2(g)} \quad (2)$$

The Gibbs free energies for reactions (1) and (2) are calculated using the standard thermodynamic data reported in Ref. [13,14]. The Gibbs energy values indicate that reaction (1) is more energetic favorable than reaction (2), which is also confirmed by the XRD analysis. Table 2 shows the corresponding quantitive values of the crucibles' XRD

Table 2
The quantitative XRD results of oxidized crucibles, both types, at 1200 °C.

[%]	Type A	Type B
α-Si_3N_4	70.90	69.96
β-Si_3N_4	28.72	28.97
SiO_2	0.38	1.05
Si_2ON_2	0	0

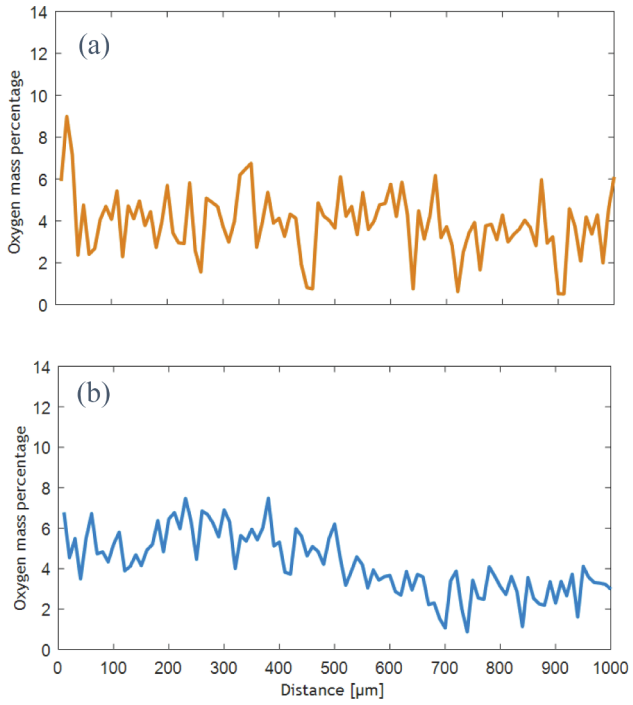

Fig. 6. Oxygen profile for crucible A: (a) inner surface- bulk, (b) outer surface-bulk.

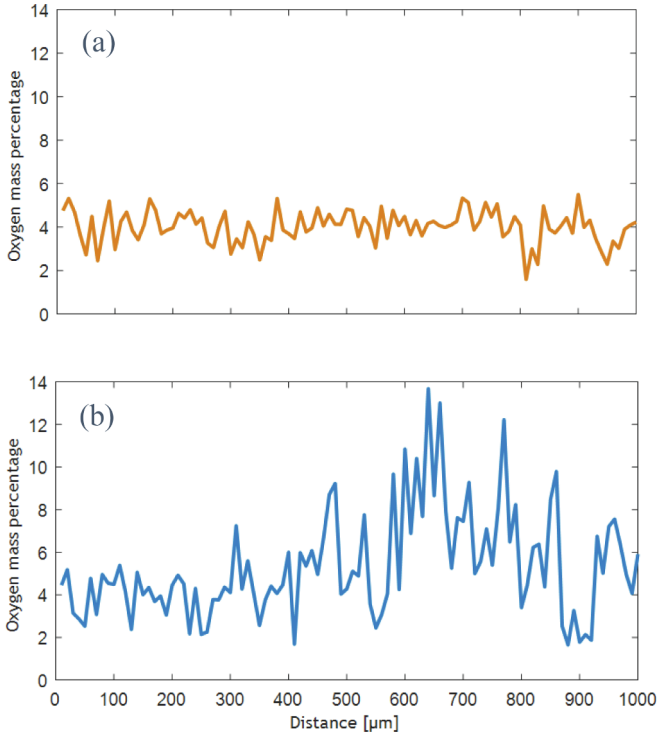

Fig. 7. Oxygen profile for crucible B: (a) inner surface- bulk, (b) outer surface-bulk.

patterns after oxidation at 1200 °C. Higher silica content is found in Type B while Si_2ON_2, in both types, is below the detection level of XRD. Crucible A shows high oxidation resistance due to its less porous

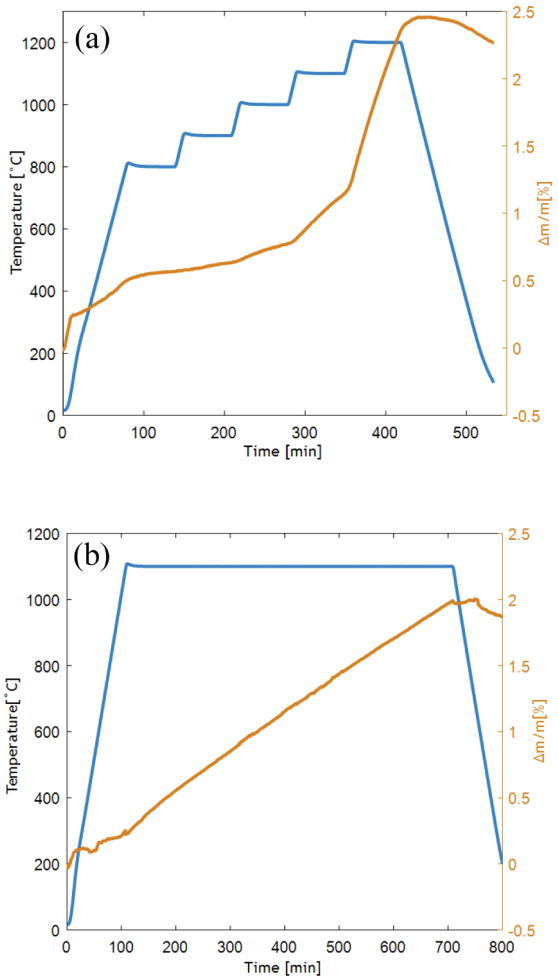

Fig. 8. Oxidation of type B: (a) between 800 °C and 1200 °C, and (b) 700 min at 1100 °C.

structure compared to type B. Yet the oxide products distribution which reflects the samples' oxidation depth is not revealed by XRD. To investigate the oxygen penetration inside the crucibles, EPMA is conducted on cross-sectional surfaces of the oxidized crucible as presented in Figs. 6 and 7. The line scanning is performed along 1 mm towards the bulk from the inner and the outer surfaces. Comparable oxygen values are observed along 1 mm from the inner surface towards the bulk for both types which goes also in line with the porosity profile both crucibles. The oxygen values fluctuate slightly around its average value along the scanned line but no significant decrease, in the oxygen profile, is observed. On the other hand, the oxygen profile along 1 mm from the outer surface of both types is not similar. Type A shows a decrease in the oxygen content from the outer surface towards the bulk while the oxygen values increase at, approximately, 500 μm from the outer surface in type B. Such a contrast, between A and B types, reflects the difference in the porosity distribution from the outer surface towards the bulk in both types. In principle, as described by Proz and Thümmler [12], the oxidation reaction must be restricted to the outer surface due to the pore sealing by oxide products and thus the oxygen content decreases away from the surface. This can fairly explain the oxidation behavior shown in Fig. 6 (b). But the oxygen profile in Fig. 7 (b) does not follow the same trend. Sealing the outer surface means hindering the oxygen diffusion inside the pores however this process is

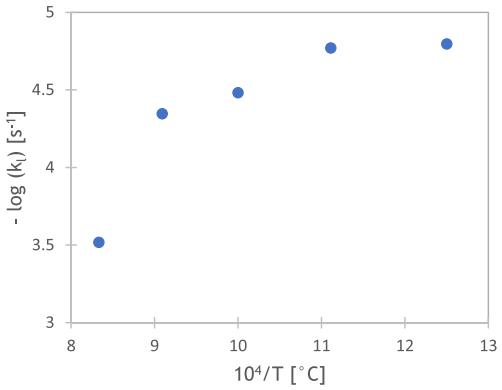

Fig. 9. Arrhenius plot of the linear rate coefficient for crucibles type B.

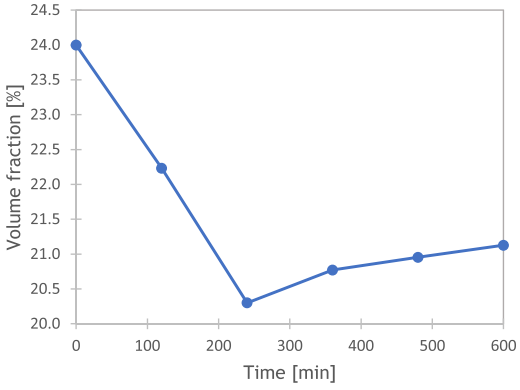

Fig. 10. Volume fraction of the open porosity during oxidation at 1100 °C.

Table 3
The corresponding quantitative results of XRD patterns in Appendix (Fig. 2).

[%]	Bulk before oxidation	5.5 mm layer from inner surface (bulk)	0.7 mm layer from outer surface
α-Si_3N_4	70.12	63.47	90.76
β-Si_3N_4	29.77	34.58	8.85
SiO_2	0.11	1.95	0.39

controlled by the balance between oxygen consumption by the oxidation reaction and the oxygen diffusion to the reaction interface. Porz and Thümmler [12] describe the oxygen diffusion inside the pores by Knudsen diffusivity model [15] assuming that the mean free path of the pore is much larger than its radius and hence the oxygen molecules bouncing with the pore walls is further likely than colliding between each other. The latter assumption is limited to very small pore radius; up to 100 nm. Therefore, Knudsen diffusivity model cannot be used to describe the oxidation behavior that shown in Fig. 7 (b) because of the following:

(i) Porosity distribution: the porosity profile is not comparable across the crucibles thickness as illustrated in Fig. 5.
(ii) Pores size: the mean pore channel radius in the bulk, for both types, is approximately 180 nm, however, the mean pore radiuses in the outer surface of the crucibles are 1.01 and 1.32 μm for types A and B respectively.

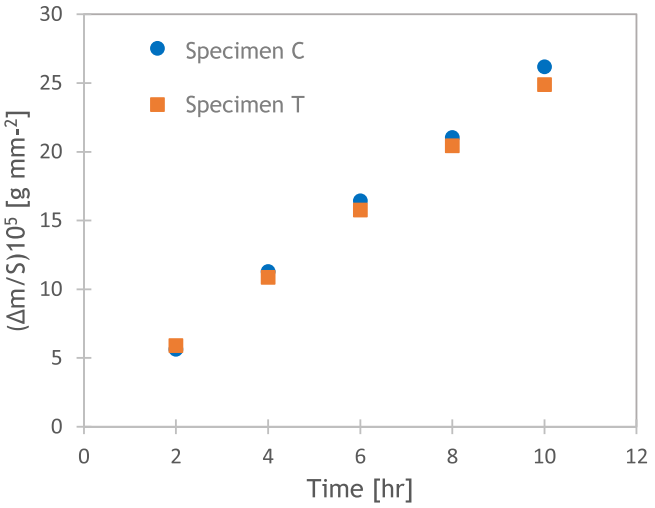

Fig. 11. Normalized mass gain of two specimen sizes vs isothermal oxidation duration at 1100 °C. Specimen C is RBSN crucible (ø 250 mm), and specimen T is (0.5x0.5x10 mm^3); TG/DTA specimen.

Turning to the oxidation reaction inside the pore which is the major contributor to the pore sealing. The oxidation of silicon nitride is combined with a mass gain (see Equation (1)). TG/DTA is conducted on type B to better understand the oxidation behavior at different temperatures. Fig. 8 (a) shows the mass gain, as a function of time and temperature. Thermal analysis is applied by heating the sample to 1200 °C and holding for one hour every 100 °C between 800 °C and 1200 °C to investigate the mass gain at each interval. Obviously, there is a linear dependence relationship between the mass gain and the time at constant temperature which is also confirmed by the isothermal oxidation shown in Fig. 8 (b). This linear behavior is consistent with other researches [12,16,17] which report two oxidation regimes of RBSN; initial linear oxidation followed by a parabolic behavior which results by the silica formation in the outer surface. Therefore, at relatively short oxidation periods as in the case of the crucibles heat treatment, the linear regime dominates the isothermal oxidation. But the oxidation rate is strongly influenced by the temperature as shown in Fig. 9 which provides the temperature dependence of the linear oxidation coefficients. The total mass gained at 1100 °C is 2% , within the linear regime, however, similar value is reported as the final mass gain , within the parabolic regime , in Ref [12]. The parabolic regime, time constant, is not observed within the oxidation cycles of the crucible before cracking. The absence of the time constant regime, in which the final mass gain is reached, indicates that pore sealing model is not applicable in this case. Evans [18] formulates the time constant based on the self-sealing pore which assumes that oxygen uptake reduces with time as the open porosity fraction decreases. To check the validity of this assumption, we measure the open porosity fraction during isothermal oxidation at 1100 °C as shown in Fig. 10. The plot shows two main regimes: (i) steep decrease in the open porosity fraction during the first four hours, (ii) steady and relatively high fraction (21%) till the completion of the experiment. Therefore, the assumption of self-blocking pores mechanism, limited to very small pores size, 100 nm, and is not applicable in the case of RBSN crucibles. Further investigations on Type

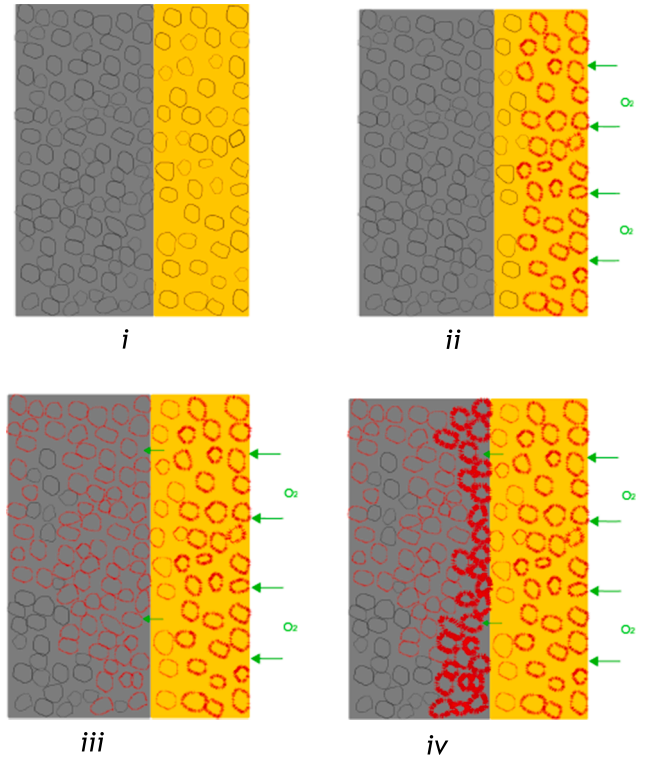

Fig. 12. Schematic illustration of the oxidation mechanism that lead to cracking of crucible type B. Yellow represents the outer surface; relatively high porosity and high content of α-Si_3N_4. Grey represents the bulk; relatively low porosity and lower content of α-Si3N4 compared to the bulk. Red represents the oxide layer.

B are introduced below to better understand the oxidation behavior of the outer surface that leads to cracking.

A significant parameter that must be considered is the phase distribution across the crucible thickness. The ratio of both polymorphic structures α and β in the RBSN crucibles is approximately 70:30. However, we investigate the phase distribution homogeneity across the thickness as shown in Appendix (Fig. 2) and the corresponding quantitive values in Table 3. The outer layer, 0.72 mm from the outer surface, reveals higher content of α-Si_3N_4 and a lower SiO_2 content, compared to the bulk. The low oxide content in the outer surface agrees with the oxygen mapping results in Fig. 7(b). It is worth noting that Ricoult et al. [16] report higher oxidation resistance of α-Si_3N_4 compared to β-Si_3N_4. It is therefore likely that such low oxygen content in the outer surface of oxidized crucibles B is due to being rich in α-Si_3N_4. The difference in the oxygen profile between the outer and the inner surfaces of crucibles Type B is not just linked to the porosity values, but also to the phase distribution in these regions.

Unlike most of the previous studies [12,16,19–21], the oxidation tests are carried out on two sizes of specimens; industrial scale ; crucibles, and lab scale ; TG/DTA samples . To compare the oxidation behavior of both geometries and to check whether the TG/ DTA samples can represent the oxidation of large crucibles, same thermal cycles are applied as shown in Fig. 11. The mass gain is normalized to the samples' surface areas and plotted versus time. Same mass gain values per unit area are obtained for both specimens' types which indicates same oxidation behavior of both types regardless of the geometry.

Based on the results above, we suggest a possible oxidation mechanism that leads to the crucibles failure as presented in Fig. 12 and explained as follows:

I. The main characteristics of the outer surface which significantly contribute to its oxidation behavior are high volume fraction of open porosity (~20%) and high content of α-Si_3N_4. Consequently, the oxidation of the outer surface occurs in two main steps:
   i. Relatively high oxidation rate at early stage which can explain the steep decrease in the open porosity (%) during oxidation, see Fig. 9. This step is mainly controlled by the gas–solid reaction that presented in Equation (1).
   ii. Extremally slow or nonexistent oxidation process resulting in steady open porosity fraction with time as presented in Fig. 10. The oxygen diffusion into the oxide layer is the rate-determining step at this stage.

II. The interconnected pores promote the oxygen penetration to the bulk which in turn induces the internal oxidation. The oxidation rate is higher than in step (i) owing to the high content of β-Si_3N_4 in this region which shows less oxidation resistance as mentioned before. This explains the high oxygen percentage towards the bulk, see Table 3 and Fig. 7(b).

III. Internal oxidation of the RBSN leads to accumulation of oxide products in the bulk as illustrated in Fig. 12 (iv) which can cause thermal stresses, during cooling, due to the high thermal expansion mismatch between the matrix and its oxides. Consequently, the crucible experience severe cracking that peels off the outer surface as shown previously in Fig. 4.

4. Conclusions

The crucible heat treatment is a limiting factor to the number of its runs, as it must precede each solidification run and it contributes to the oxide accumulation in the entire crucible. At a certain threshold of the internal oxide content, crucibles crack due to the severe thermal stresses. The relatively high oxidation rates of the crucibles reduce the time to reach the threshold and hence the number of runs. Developing a passive oxide film on the outer surface of the crucible can hinder the oxygen penetration to the bulk, and hence the internal oxidation. Yet promoting the external oxidation, over the internal oxidation, is strongly influenced by: (i) the porosity's amount, size and distribution, and (ii) the phase distribution across the thickness. As the crucibles' open porosity is characterized by a high-volume fraction and large size of pores, it precludes sealing the outer surface before cracking.

Acknowledgment

The work reported in this paper was performed in crucibles for next generation high quality silicon solar cells (CRUGENSI), project no.: 268027/E20 funded by the Norwegian Research Council's and industry partners.

Appendix

(See Fig. A1).

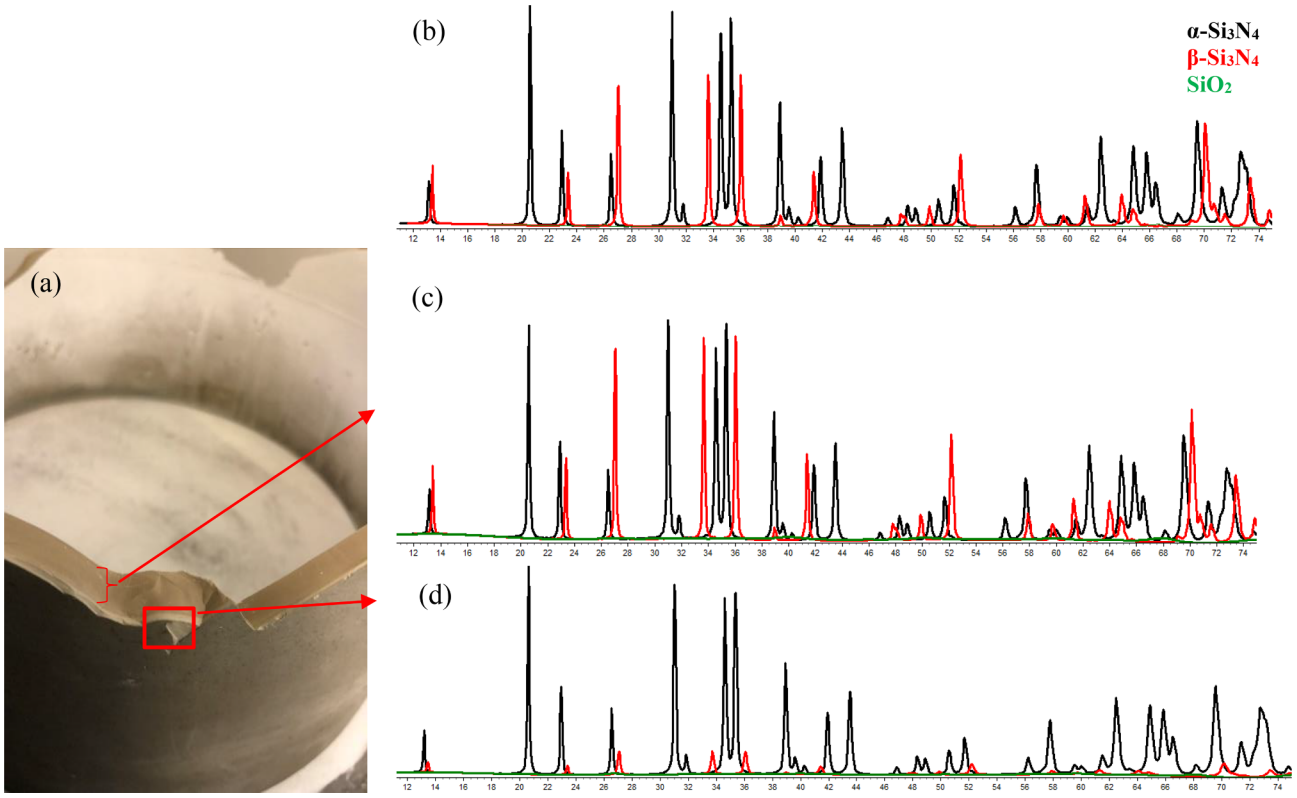

Fig. A1. (a) photograph of a broken RBSN crucible type B upon heat treatment at 1200 °C, its corresponding XRD patterns before and after oxidation; (b) bulk before oxidation, (c) 0.72 mm layer from the outer surface, and (d) 5.5 mm layer from the inner surface. Black spectra represent α-Si_3N_4, red for β-Si_3N_4 and green for SiO_2.

References

[1] M.P. Bellmann, et al., Crystallization of multicrystalline silicon from reusable silicon nitride crucibles: Material properties and solar cell efficiency, J. Cryst. Growth 504 (2018) 51–55.
[2] M.C. Schubert, et al., Impact of Impurities From Crucible and Coating on mc-Silicon Quality-the Example of Iron and Cobalt, IEEE J. Photovoltaics 3 (4) (2013) 1250–1258.
[3] F. Schindler, et al., Solar Cell Efficiency Losses Due to Impurities From the Crucible in Multicrystalline Silicon, IEEE J. Photovoltaics 4 (1) (2014) 122–129.
[4] C. Khattak, F. Schmid, Reusable crucible for silicon ingot growth, Crystal Systems Inc, USA, 2003.
[5] Roligheten, R., G. Rian, and a.S. Julsrud, Reusable crucibles and method of manufacturing them, W.I.P. Organization, Editor. 2007.
[6] V. Schneider, et al., Nitride bonded silicon nitride as a reusable crucible material for directional solidification of silicon, Cryst. Res. Technol. 51 (1) (2016) 74–86.
[7] B. Drevet, O. Pajani, N. Eustathopoulos, Wetting, infiltration and sticking phenomena in Si 3N 4 releasing coatings in the growth of photovoltaic silicon, Sol. Energy Mater. Sol. Cells 94 (3) (2010) 425–431.
[8] V. Schneider, C. Reimann, J. Friedrich, Wetting and infiltration of nitride bonded silicon nitride by liquid silicon, J. Cryst. Growth 440 (2016) 31–37.
[9] F.L. Riley, Reaction Bonded Silicon Nitride, Mater. Sci. Forum 47 (1991) 70–83.
[10] K. Kazakyavichyus, et al., Thermal shock resistance of silicon nitride ceramics, Strength Mater. 20 (11) (1988) 1477–1480.
[11] B. Drevet, et al., Wetting and adhesion of Si on Si3N4 and BN substrates, J. Eur. Ceram. Soc. 29 (11) (2009) 2363–2367.
[12] F. Porz, F. Thümmler, Oxidation mechanism of porous silicon nitride, J. Mater. Sci. 19 (4) (1984) 1283–1295.
[13] Thermodynamic Properties of Compounds, Ta2N to NbO: Datasheet from Landolt-Börnstein - Group IV Physical Chemistry · Volume 19A4: "Pure Substances. Part 4 _ Compounds from HgH_g to ZnTe_g" in SpringerMaterials (https://doi.org/10.1007/10688868_12). Springer-Verlag Berlin Heidelberg.
[14] Thermodynamic Properties of Compounds, SbO2 to Rh2O3: Datasheet from Landolt-Börnstein - Group IV Physical Chemistry · Volume 19A4: "Pure Substances. Part 4 _ Compounds from HgH_g to ZnTe_g" in SpringerMaterials (https://doi.org/10.1007/10688868_15). Springer-Verlag Berlin Heidelberg.
[15] D.D. Do, Adsorption Analysis : Equilibria and Kinetics, Imperial College Press, London, 1998.
[16] M. Backhaus-Ricoult, et al., High-Temperature Oxidation Behavior of High-Purity alpha -, beta -, and Mixed Silicon Nitride Ceramics, Journal of the American Ceramic Society (USA) 85 (2) (2002) 385–392.
[17] B.E. Deal, A.S. Grove, General Relationship for the Thermal Oxidation of Silicon, J. Appl. Phys. 36 (12) (1965) 3770–3778.
[18] U.R. Evans, The corrosion and oxidation of metals : scientific principles and practical applications, Arnold, London, 1960.
[19] T. Sato, et al., High-temperature oxidation of silicon nitride-based ceramics by water vapour, J. Mater. Sci. 22 (7) (1987) 2635–2640.
[20] M. Maeda, et al., Oxidation behaviour of silicon nitride under cyclic and static conditions, Ceram. Int. 15 (4) (1989) 247–253.
[21] S.P. Taguchi, S. Ribeiro, Silicon nitride oxidation behaviour at 1000 and 1200 °C, Journal of Materials Processing Tech. 147 (3) (2004) 336–342.